Journal of Infectious Diseases Advance Access published July 3, 2015

Antigenic maps of influenza A/H3N2 virus produced with human antisera obtained after primary infection

Judith M. Fonville*[,1,2,3], Pieter L. A. Fraaij[3,4], Gerrie de Mutsert[3], Samuel H. Wilks[1,2], Ruud van Beek[3], Ron A. M. Fouchier[3], Guus F. Rimmelzwaan[3]

[1]Centre for Pathogen Evolution, Department of Zoology, University of Cambridge, Cambridge CB2 3EJ, United Kingdom

[2]WHO Collaborating Center for Modeling, Evolution, and Control of Emerging Infectious Diseases, Cambridge, United Kingdom

[3]Department of Viroscience, Erasmus MC, 3015 CE Rotterdam, The Netherlands

[4]Department of Pediatrics, Erasmus MC-Sophia, 3015 CN Rotterdam, The Netherlands

*Corresponding author contact information: Dr. Judith M Fonville; Center for Pathogen Evolution, Department of Zoology, University of Cambridge, CB2 3EJ, Cambridge, United Kingdom. Fax: +44 1223336676; telephone +44 1223330933; email: jmf77@cam.ac.uk

Abstract:

Background: Antigenic characterization of influenza viruses is typically based on hemagglutination inhibition (HI) assay data of viral isolates tested against strain-specific post-infection ferret antisera. Here, similar virus characterizations were performed using first-infection human rather than ferret serology data.

Methods: We screened sera collected between 1995 and 2011 from children between 9 and 24 months of age for influenza virus antibodies, performed HI tests for the positive sera against 24 influenza viruses isolated between 1989 and 2011, and measured HI titers of 24 A/H3N2 ferret sera against the same panel of viruses.

Results: Of the 17 positive human sera, 6 were high-responders, showing HI patterns that would be expected from primary infection antisera, while 11 sera had lower, more dispersed patterns of reactivity that are not easily explained. The antigenic map based on the high-responder human HI data was similar to the results using ferret data.

Conclusions: Although the overall structure of the ferret and human antigenic maps is similar, local differences in virus positions indicate that the human and ferret immune system might see antigenic properties of viruses differently. Further studies are needed to establish to what degree of detail ferret data provide equivalent patterns to human serological reactivity.

Background:

Influenza viruses are notorious for their continuous antigenic evolution, and the resulting ability to escape prior immunity and re-infect previously exposed hosts [1,2]. To protect against influenza virus infection, an effective vaccine is available, but to maintain vaccine effectiveness, the antigenic properties of circulating viruses need to be known, and the vaccine strains have to be updated when appropriate to avoid antigenic mismatch [3,4]. To this end, the World Health Organization (WHO) coordinates a global influenza surveillance network that routinely characterizes the antigenic properties of isolated viruses, using the hemagglutination inhibition (HI) assay [5]. For antigenic characterization, sera from a panel of ferrets that were each experimentally infected with a different virus strain are used. The resulting HI tables contain serum antibody titers with patterns that are now fairly readily interpretable and understood, because antigenic differences among virus strains can be mapped with antigenic cartography [1]. An antigenic map quantifies and displays antigenic differences as distances between viruses, such that similar viruses cluster closely on the map, whereas viruses that are antigenically different are found further away. This methodology is now routinely used to assist the vaccine strain selection process and surveillance activities of the WHO, and is based on large HI tables of influenza virus isolates that were titrated against a panel of ferret sera.

Although human sera are used in the vaccine strain selection process, for example to evaluate the response to vaccines in vaccine trials, they are too complicated to be trivially used in the antigenic characterization of influenza viruses. For example, when a human has had two separate exposures, titers will be increased to both infecting viruses, which may potentially be interpreted incorrectly as an antigenic similarity between the two different infecting viruses. A recent solution to the interpretation of human serological data is the antibody landscape, which expands an antigenic map in another dimension, where the extra dimension displays the HI titers measured for the human serum for each virus [6].

In addition to the fact that human data are typically representative of multiple exposures, there are manifold other reasons why ferret data are preferred for the antigenic characterization of virus isolates, often as a result of experimental control: the exact infecting virus strain for a ferret is always known, whereas for human infections this is much less common; ferret serum samples can be obtained at a standardized time point after infection, when there is a peak in antibody titers, increasing the sensitivity of interpretations of the resulting HI tables; sufficiently large serum volumes for extensive and repeated testing are available; and sera can be newly generated against viruses that circulated in the past.

The traditional interpretation of ferret HI data when performing antigenic characterization, the WHO vaccine strain selection process, and the expansion of a ferret-based antigenic map into an antibody landscape all

implicitly assume that antigenic characteristics are similar to what would be measured in a human, when using the ferret animal model. Interestingly, a small comparison of titers from swine sera and ferret sera gave similar results for swine A/H3N2 influenza virus strains [7], and the antigenic characterization of avian A/H5N1 influenza viruses using ferret sera was consistent with titer patterns in HI tests with avian antisera [8,9]. Similarly, it is important to carefully compare and know the antigenic properties of human viruses in relation to the human immune system and antibody response. To the best of our knowledge, validation studies to confirm the use of the ferret as a model system for the antigenic characterization of seasonal influenza isolates in the context of different human immune responses have not been performed. This is understandable, because it is challenging to obtain sera that fulfill the stringent requirements of first-infection human sera of enough volume that were obtained from individuals during the circulation of different antigenic clusters.

This study presents the first human antigenic map made for influenza viruses, and is based on a data set of historic and recent serum samples, to enable antigenic characterization of various influenza A/H3N2 isolates recognized by human antibody repertoires. By having access not only to recent, but also to historical children's serum samples, we were not limited to characterization of a small subset of recently circulating viruses. Instead, our analysis investigated serum responses against viruses isolated over 22 years of influenza A/H3N2 virus evolution, across 9 antigenic clusters. These data enable a comparison of antigenic properties of viruses defined by human sera

after natural infection to those defined by ferret sera obtained after experimental infection.

Methods:

Human serum samples were selected from the serum bank of the Department of Viroscience at the Erasmus Medical Centre (Rotterdam, NL). Only sera of patients seen at the Sophia Hospital Pediatrics ward who, and of whom the caregivers, did not object to scientific use of excess material were included in this study. The study protocol was reviewed and approved by the medical ethics board of the Erasmus University Medical Center (study number MEC-2012-181). Informed consent was waived because patient inclusion was performed retrospectively and data handled anonymously. From the 5129 individuals, we selected individuals of 270-729 days old, to minimize interference from transplacentally acquired maternal IgG antibodies (IgA antibodies in breastmilk were not considered relevant for our studies of sera), or multiple seasonal influenza virus infections [10,11]. We excluded sera from patients in whom the possibility of non-naturally obtained antibody response existed, and samples from patients with immune deficiencies were also excluded. Based on surveillance data of influenza A/H3N2 incidence in the Netherlands, we selected samples that were collected within two weeks either side of the epidemic season window. We then selected samples with at least 150 µL serum, leading to a final sample set of 72 sera (see **Supporting Methods**).

Hemagglutination inhibition (HI) assays were used to screen the serum samples for influenza virus-specific antibodies against the vaccine strain for the antigenic cluster that circulated in that season (see **Supporting Dataset S1**), using the standard protocol [12,13]. The 17 influenza virus-positive samples were subsequently tested further with HI against a panel of 23 viruses (see **Supporting Dataset S2**). **Table S1** lists the frequencies for the various reasons for hospitalization and diagnostic testing of these 17 patients, of whom four had underlying medical conditions (congenital kidney disease, bone formation disorder, neonatal cataract and recurrent wheezing). For comparative purposes, we tested the sera of 24 ferrets against the same panel of viruses with the HI assay. **Supporting datasets S3-S7** show the HI results and subsets used for antigenic cartography, see **Supporting Methods**.

Antigenic maps were used to infer antigenic differences among virus strains, where each titer in the HI table specifies a target distance for the virus and serum points in the antigenic map [1].

Antibody landscapes were constructed as described in Fonville *et al.* [6], except for a modification to model the effects of the x and y antigenic coordinate variables independently, see **Supporting Methods**.

Results:

We selected sera from a biobank of samples collected and stored from children between the ages of 9 and 24 months of whom blood was drawn for any viral diagnostic analysis between 1995 and 2012. Upon screening the 72 selected sera against influenza virus-specific antibodies with the HI assay, 17 had an HI titer of 10 or higher against the screening virus (23.6%). Interestingly, there was a dichotomy in the HI screening titers, with one group of relatively high-responding individuals (n = 6, HI titer range against screening virus 240-3840, 8.3% of all sera screened), and a group of low-responders (n = 11, HI titer range against screening virus 10-60), see **Supporting Dataset S2**.

The 17 influenza virus-positive human sera and 24 ferret sera were subsequently titrated with HI against a panel of viruses. **Figure 1** visualizes the resulting HI titer patterns, where viruses were color-coded by the antigenic cluster as determined from previously published antigenic maps based on ferret sera [1,6]. Evolution of influenza A/H3N2 viruses since its introduction in 1968 has included the addition of glycosylation sites [14,15]. Although the shielding of epitopes by glycans has been reported frequently to alter or prevent the ability of neutralizing antibodies to bind the virus by masking or modifying antigenic sites [16,17], we do not see significant changes in the number of antigenic clusters recognized by sera over time, in line with the lack

of synchronicity between antigenic cluster transitions and changes in glycosylation [18].

Figure 1 highlights how titers between sera and viruses that are many years apart (long-distance titers) are more common for the human sera than for the ferret sera: first infection sera of the three low-responders in 1995 (S95-2, S95-3, S95-4), for example, show titers up to strains isolated in 2011, whereas such patterns are uncommon in the ferret data. Similarly, S10-2 and S11-1 show titers to strains that circulated around two decades before the child was born. Although some serum-virus combinations in the ferret data show numeric titers where they would not be expected, this is a more common feature in the human data, particularly in the sera of low-responders. In general, the ferret sera appear to show stronger and narrower patterns of reactivity than the human sera.

We proceeded by focusing our analyses on the sera of the high-responders, and generated an antigenic map based on these six sera S95-1, S00-1, S00-2, S04-1, S04-2 and S04-3 (see **Supporting Dataset S4**). The number of viruses per antigenic cluster can vary and still result in robust antigenic maps, as long as the density of viruses is high enough. Viruses can be placed reliably on a map once there are numeric titer values against at least two sera, and we mapped the eligible 14 viruses, isolated between 1992 and 2011. **Figure 2** displays the resulting antigenic map, with viruses colored by antigenic cluster and antisera colored by the antigenic cluster that was present in the season the sample was obtained. Interestingly, the viruses

mostly still cluster by color, i.e. the assignment to antigenic clusters based on ferret sera reactivity matches fairly well with the human antigenic map. The antigenic map represents the measured HI data well, as characterized by small error lines (see **Supporting Figure S1**).

The human sera are relatively close to the viruses for the corresponding antigenic cluster, with the possible exceptions of S04-1 and S04-2. The individual S04-1 may have been infected before the 2003/2004 season, in the 2001/2002 season (although high levels of maternal antibodies would be expected for an individual this soon after birth), or in the 2002/2003 season, when the relatively small influenza epidemic in the Netherlands was dominated by strains that were antigenically like the Sydney-97 antigenic cluster [19]. An infection with a Sydney-97-like virus would explain the location of this serum in the antigenic map close to such isolates. The S04-2 serum is antigenically slightly more advanced than the surveillance data for the 2003/2004 influenza season in the Netherlands [20], and similar to the California-04-like viruses that circulated during the 2004/2005 epidemic [21]. **Supporting Figure S2** shows a similar map made of the children's HI data, made with a column basis of at least 1280 (conventionally used for the analysis of ferret serology), and underlines how the antigenic relationships and positions of the sera are similar for both analyses.

Importantly, we can compare the positioning of the viruses on the antigenic map as defined by the human sera with an antigenic map based on ferret sera. **Figure 3A** shows an antigenic map of 21 ferret sera (see **Supporting**

Dataset S5) measured against the same subset of viruses, and **Figure 3B** displays “procrustes” arrows, where the arrowhead indicates the corresponding positions of the viruses in the human map. Although the overall structure of the two maps remained similar, in terms of relative ordering of antigenic properties (where e.g. the Beijing-1992 and Wuhan-1995 clusters are closer to each other than to the California-2004 cluster), there are visible differences between the two maps. Additionally, the overall spread of the antigenic map comprises fewer antigenic units when based on human sera, than based on ferret sera. Similar observations were made when comparing the human and ferret maps made with the minimum column basis requirement, see **Supporting Figure S3**, and when making the ferret map based on a subset of six sera only (**Supporting Figure S4**).

Subsequently, we explored how the human antigenic map would change when two of the low-responders are included (these sera had at least one titer of at least 240, instead of the screening titer being at least 240), see **Supporting Dataset S6**. The resulting map, shown in **Figure 4A**, is quite comparable to the antigenic map made without these two sera: the procrustes arrows in **Figure 4B** are relatively small, with the exception of a large change in the position of virus VI/361/11. The new addition of viruses VI/1/89 and PE/16/09 causes the appearance of the map to become circular, as a result of some long-distance cross-reactivity of some of the recent sera against VI/1/89 pulling this virus inwards. The ferret map made with the same subset of viruses (**Figure 4C**, **Supporting Dataset S7**) also has a moderately circular appearance, but is spaced more widely, compared to the human map (see the

procrustes arrows in **Figure 4D**). In general, broader reactivity will typically result in antigenic maps becoming more circular than linear.

To visualize the titer pattern of an individual's serum, we added an extra dimension to the antigenic map to display the measured HI titers. By plotting a smooth surface through these titers, an antibody landscape is created, which plots the antibody recognition patterns as a function of the antigenic relationships among viruses [6]. **Figure 5** displays the antibody landscapes of the six sera, where each landscape represents an individual's antibody profile, with elevations corresponding to regions in the antigenic map with higher antibody levels, and depressions to regions with lower antibody reactivity. These antibody landscapes are the first ones made for first-infection human sera, and the first ones made on a human-serum based antigenic map. When comparing the antibody landscapes of the human sera with the landscapes of the most similar ferret sera, the landscape shapes are remarkably similar (see **Supporting Figure S5**).

Discussion:

This study evaluated the HI titer patterns of 17 sera from children between 9 and 24 months of age. HI titers after primary infection in the literature vary widely, and are known to be dependent on the time of serum collection after infection [22–26], but also possibly the virus subtype [22,27] and age of the individual [28,29]. Some studies in the literature follow individuals from birth [24,30], and hence have certainty about an infection being a primary

exposure, while other relevant studies report titers for age groups that are typically associated with first infection [10,22,28,31–35].

Two studies that report titers after primary infection with A/H3N2 are Wright *et al.*, reporting a geometric mean titer (GMT) of 271 based on 8 children between 6 and 23 months old [22], and Burlington *et al.* reporting a GMT of 147 based on 10 children between 1 and 4 years of age, followed from birth [30]. In the Pienter study [10], titers of children between 12 and 24 months had a GMT against A/H3N2 viruses of 329. These values are in line with the high titers we find in the sera of high-responders.

The reason for the titer patterns observed in the low-responding individuals remains unclear. Although the timing of the sample draw in relation to any influenza virus infection is unknown and will vary from person to person, there was no difference between the low-responder and high-responder group for the moment of the sample draw in relation to the dates of that season's epidemic. The sera of the low-responders did not have the same reactivity patterns as the high-responders with simply lower HI values, but instead showed more dispersed reactivity patterns. Subclinical infection or antigen exposure, which would potentially lead to lower HI titers [36], do not explain these odd reactivity patterns. Sometimes these titers extended to many antigenic clusters before the child was born, or indeed to many antigenic clusters that circulated after the serum collection. Maternal antibodies might be able to explain the former, but not the latter observation. Moreover, we had a fairly conservative selection criterion (aged over 9 months) to avoid

detection of maternal antibodies as much as possible, and the age ranges were similar in the low- and high-responder groups. The dispersed reactivity patterns could possibly be the result of the existence of natural antibodies. Alternatively, these patterns might also arise through cross-reactivity with antibodies induced after infections with other pathogens, such as other influenza viruses, or even non-influenza pathogens, which is likely in children of this age group, but not in specific-pathogen-free ferrets. Further studies are necessary to investigate the cause of the patterns seen in the low-responders, and will require the collection of a larger serum volume for testing.

We have, for the first time, constructed an antigenic map of influenza viruses based on human antibody recognition data. This antigenic map was based on an extensive set of human HI titers, spanning both a long time range of serum sampling, and comprising two decades of evolution in the influenza virus test strains. Our data, and in particular the antibody landscapes, also illustrate the antibody response in terms of strength, but also breadth, in children after their first infection, across a range of different infecting strains and seasons. It would be very interesting to study how this response changes as an individual would experience its second, and third infection, to investigate how the antibody landscape of an individual is built up over time [6]. Indeed, in the context of vaccine strain selection, a previous exposure history might alter the antibody landscape and thus the immune response in a such way that data from primary infection antisera-based antigenic maps may not provide the best possible protection against influenza viruses for not-naïve individuals [6,37,38].

The human antigenic map was based on six high-responding human sera, and is therefore by definition less robust than the ferret map based on 21 ferret sera. For example, the larger symbol sizes in **Figure 2** for the more recent virus isolates indicate relatively larger uncertainty in the positioning of these viruses, and is a natural result of fewer and lower numeric titers against those strains, because the sera were only from older influenza seasons. When including more recent sera, as in **Figure 4**, the uncertainty in the positioning of the more recent viruses therefore decreased. However, even when making a map of six ferret sera only (**Supporting Figure S4**), the ferret map spanned a larger antigenic range than the human antigenic map. This may be caused by the fact that inoculation protocols and serum collection for ferrets have been optimized to yield high titers.

The first-infection human sera are similar, but not identical, to the ferret sera, which were obtained under controlled conditions. For example, the sample collection of ferret sera is standardized at two weeks post-infection, whereas the time between infection and sample collection is unknown for the human sera. We did try to minimize variation in the time post-infection in the human sera by only selecting samples drawn in a narrow window around the epidemic in the Netherlands for each season, but are still limited by the absence of information on infection history. Additionally, whereas the infecting strain is known for ferret sera, this information was not available for the human sera, and some children may have been infected in a season preceding the season during which the serum was drawn. Another potential

difference between the ferret and children sera is that the route and dose of infection is standardized and known for the ferrets, but might have varied for the children; similarly, the ferrets were infected with laboratory-passaged viruses, whereas the children were exposed to unpassaged circulating virus. Finally, the immunological maturity between the young adult ferrets and the 9-24 months old children might be different.

Despite these differences between the experimentally obtained ferret sera and human sera obtained under less-controlled conditions, the ferret and human maps are globally similar, indicating that the ferret sera are able to detect useful information on overall antigenic differences among virus strains. However, the narrower spacing of the human map compared to the ferret antigenic map, and the differences in the local positioning of the viruses between the maps may be relevant. Therefore, a carefully planned prospective experiment where a larger number of human sera are obtained at known times post-infection is warranted to further test these differences. The germline B-cell receptor repertoires may be different between humans and ferrets, which would lead to different antibody mixtures. If the human and ferret antibodies would respond to different epitopes on the hemagglutinin, antigenic maps would be different as a result. In case the different positioning is truly caused by differences in how antigenic properties are detected by ferret versus human immune systems, and relevant to vaccine strain selection, it might be helpful to supplement the ferret data with first-infection human sera.

Funding statement:

This work was supported by the award of a Fellowship in Biomedical Informatics from the Medical Research Council UK [grant number MR/K021885/1] and a Junior Research Fellowship from Homerton College Cambridge to J.M.F.; a Medical Research Council UK studentship [number MR/K50127X/1 to S.H.W.]; the EU FP7 project PREPARE [grant number 602525 to P.L.A.F.]; the National Institute of Allergy and Infectious Diseases, National Institutes of Health [contract number HHSN272201400008C to R.A.M.F and the Center for Pathogen Evolution]; and the EU grant FLUNIVAC [grant number 602604 to G.F.R.].

Conflict of interest statement:

P.L.A.F. and R.A.M.F. participate in the IRIS trial sponsored by Hoffmann-La Roche. G.F.R. is employed as a consultant by Viroclinics Biosciences B.V.

Acknowledgements:

We would like to thank Björn Koel, Leah Katzelnick and Derek Smith for helpful discussions.

References:

1. Smith DJ, Lapedes AS, de Jong JC, et al. Mapping the antigenic and genetic evolution of influenza virus. Science **2004**; 305:371–6.
2. Bush RM, Fitch WM, Bender CA, Cox NJ. Positive selection on the H3 hemagglutinin gene of human influenza virus A. Mol Biol Evol **1999**; 16:1457–65.
3. Carrat F, Flahault A. Influenza vaccine: The challenge of antigenic drift. Vaccine **2007**; 25:6852–62.
4. Belongia EA, Kieke BA, Donahue JG, et al. Effectiveness of inactivated influenza vaccines varied substantially with antigenic match from the 2004-2005 season to the 2006-2007 season. J Infect Dis **2009**; 199:159–67.
5. Russell CA, Jones TC, Barr IG, et al. Influenza vaccine strain selection and recent studies on the global migration of seasonal influenza viruses. Vaccine **2008**; 26S:D31–D34.
6. Fonville JM, Wilks SH, James SL, et al. Antibody landscapes after influenza virus infection or vaccination. Science **2014**; 346:996–1000.
7. de Jong JC, Smith DJ, Lapedes AS, et al. Antigenic and genetic evolution of swine influenza A (H3N2) viruses in Europe. J Virol **2007**; 81:4315–22.
8. Koel BF, van der Vliet S, Burke DF, et al. Antigenic variation of clade 2.1 H5N1 virus is determined by a few amino acid substitutions immediately adjacent to the receptor binding site. MBio **2014**; 5:e01070–14.

9. Fouchier RAM, Smith DJ. Use of antigenic cartography in vaccine seed strain selection. Avian Dis **2010**; 54:220–3.

10. Bodewes R, de Mutsert G, van der Klis FRM, et al. Prevalence of antibodies against seasonal influenza A and B viruses in children in Netherlands. Clin Vaccine Immunol **2011**; 18:469–76.

11. Irving WL, James DK, Stephenson T, et al. Influenza virus infection in the second and third trimesters of pregnancy: a clinical and seroepidemiological study. BJOG **2000**; 107:1282–9.

12. Masurel N, Ophof P, de Jong P. Antibody response to immunization with influenza A/USSR/77 (H1N1) virus in young individuals primed or unprimed for A/New Jersey/76 (H1N1) virus. J Hyg (Lond) **1981**; 87:201–9.

13. Hirst GK. The quantitative determination of influenza virus and antibodies by means of red cell agglutination. J Exp Med **1942**; 75:49–64.

14. Skehel JJ, Wiley DC. Receptor binding and membrane fusion in virus entry: the influenza hemagglutinin. Annu Rev Biochem **2000**; 69:531–79.

15. Tate MD, Job ER, Deng YM, Gunalan V, Maurer-Stroh S, Reading PC. Playing hide and seek: How glycosylation of the influenza virus hemagglutinin can modulate the immune response to infection. Viruses **2014**; 6:1294–316.

16. Skehel JJ, Stevens DJ, Daniels RS, et al. A carbohydrate side chain on hemagglutinins of Hong Kong influenza viruses inhibits recognition by a monoclonal antibody. Proc Natl Acad Sci U S A **1984**; 81:1779–83.

17. Abe Y, Takashita E, Sugawara K, Matsuzaki Y, Muraki Y, Hongo S. Effect of the addition of oligosaccharides on the biological activities and antigenicity of influenza A/H3N2 virus hemagglutinin. J Virol **2004**; 78:9605–11.

18. Blackburne BP, Hay AJ, Goldstein RA. Changing selective pressure during antigenic changes in human influenza H3. PLoS Pathog **2008**; 4:e1000058.

19. de Jong JC, Rimmelzwaan GF, Bartelds AIM, Wilbrink B, Fouchier RAM, Osterhaus ADME. Het influenzaseizoen 2002/'03 in Nederland en de vaccinsamenstelling voor het seizoen 2003/'04. Ned Tijdschr Geneeskd **2003**; 147:1971–5.

20. Rimmelzwaan GF, de Jong JC, Bartelds AIM, Wilbrink B, Fouchier RAM, Osterhaus ADME. Het influenzaseizoen 2003/'04 in Nederland met een beperkte epidemie door de virusvariant A/Fujian, en de vaccinsamenstelling voor het seizoen 2004/'05. Ned Tijdschr Geneeskd **2004**; 148:1984–8.

21. de Jong JC, Rimmelzwaan GF, Bartelds AIM, Meijer A, Fouchier RAM, Osterhaus ADME. Het influenzaseizoen 2004/'05 in Nederland met de grootste epidemie van de laatste 5 jaar, door virusvariant A/California, en de vaccinsamenstelling voor het seizoen 2005/'06. Ned Tijdschr Geneeskd **2005**; 149:2355–61.

22. Wright PF, Sannella E, Shi JR, Zhu Y, Ikizler MR, Edwards KM. Antibody responses after inactivated influenza vaccine in young children. Pediatr Infect Dis J **2008**; 27:1004–8.

23. Wang M, Yuan J, Li T, et al. Antibody dynamics of 2009 influenza A (H1N1) virus in infected patients and vaccinated people in China. PLoS One **2011**; 6:e16809.

24. Frank AL, Taber LH, Glezen WP, Paredes A, Couch RB. Reinfection with influenza A (H3N2) virus in young children and their families. J Infect Dis **1979**; 140:829–36.

25. Ng S, Fang VJ, Ip DKM, et al. Estimation of the association between antibody titers and protection against confirmed influenza virus infection in children. J Infect Dis **2013**; 208:1320–4.

26. Johnson PR, Feldman S, Thompson JM, Mahoney JD, Wright PF. Comparison of long-term systemic and secretory antibody responses in children given live, attenuated, or inactivated influenza A vaccine. J Med Virol **1985**; 17:325–35.

27. Belshe RB, Mendelman PM, Treanor J, et al. The efficacy of live attenuated, cold-adapted, trivalent, intranasal influenzavirus vaccine in children. N Engl J Med **1998**; 338:1405–12.

28. Kang EK, Lim JS, Lee JA, Kim DH. Comparison of immune response by virus infection and vaccination to 2009 pandemic influenza A/H1N1 in children. J Korean Med Sci **2013**; 28:274–9.

29. Walter EB, Rajagopal S, Zhu Y, Neuzil KM, Fairchok MP, Englund JA. Trivalent inactivated influenza vaccine (TIV) immunogenicity in children 6 through 23 months of age: Do children of all ages respond equally? Vaccine **2010**; 28:4376–83.

30. Burlington DB, Wright PF, van Wyke KL, Phelan MA, Mayner RE, Murphy BR. Development of subtype-specific and heterosubtypic

antibodies to the influenza A virus hemagglutinin after primary infection in children. J Clin Microbiol **1985**; 21:847–9.

31. Verma N, Dimitrova M, Carter DM, et al. Influenza virus H1N1pdm09 infections in the young and old: Evidence of greater antibody diversity and affinity for the hemagglutinin globular head domain (HA1 domain) in the elderly than in young adults and children. J Virol **2012**; 86:5515–22.
32. Lerdsamran H, Pittayawonganon C, Pooruk P, et al. Serological response to the 2009 pandemic influenza A (H1N1) virus for disease diagnosis and estimating the infection rate in Thai population. PLoS One **2011**; 6:e16164.
33. Slepushkin AN, Ritova VV, Feklisova LV, et al. Results of a two-year study of humoral immunity to influenza A and B viruses in children under the age of 14 years in Moscow and its suburbs. Bull World Health Organ **1984**; 62:75–82.
34. Kase T, Morikawa S, Okuno Y, Maeda A, Baba K. Reinfection with antigenically similar influenza virus observed at a pediatric clinic in Osaka from December 1998 to April 2002. Int Congr Ser **2004**; 1263:304–7.
35. Mörner A, Bråve A, Kling A-M, et al. Pandemic influenza A(H1N1)pdm09 seroprevalence in Sweden before and after the pandemic and the vaccination campaign in 2009. PLoS One **2012**; 7:e53511.
36. Meijer A, Bosman A, van de Kamp EEHM, Wilbrink B, van Beest Holle MDR, Koopmans M. Measurement of antibodies to avian influenza virus

A(H7N7) in humans by hemagglutination inhibition test. J Virol Methods **2006**; 132:113–20.

37. Li Y, Myers JL, Bostick DL, et al. Immune history shapes specificity of pandemic H1N1 influenza antibody responses. J Exp Med **2013**; 210:1493–500.

38. Linderman SL, Chambers BS, Zost SJ, et al. Potential antigenic explanation for atypical H1N1 infections among middle-aged adults during the 2013-2014 influenza season. Proc Natl Acad Sci U S A **2014**; 111:15798–803.

Figure legends:

Figure 1: Figure displaying the measured hemagglutination inhibition (HI) titer with an increasing symbol size (<10 are size zero) for the ferret sera (top) and human sera (bottom), sorted by year of isolation of the infecting virus and the year of serum draw respectively, against the viruses sorted by their antigenic cluster. Different antigenic clusters are indicated with different colors: *blue*: Sichuan-87 cluster; *red*: Beijing-89 cluster; *pink:* Beijing-92 cluster; *dark green:* Wuhan-95 cluster; *light blue:* Sydney-97 cluster; *yellow:* Fuijan-02 cluster; *light green:* California-04 cluster; *orange:* Brisbane-07 cluster; *purple:* Perth-09 cluster. See also **Supporting Dataset S2** and **S3**.

Figure 2: Antigenic map based on the hemagglutination inhibition (HI) titers of the sera of the six high-responders and representative virus isolates of different antigenic clusters [1]. In an antigenic map, both vertical and horizontal axes represent antigenic distance. The spacing between gridlines is one antigenic unit distance, corresponding to a two-fold dilution in the HI assay, 2 units correspond to a four-fold dilution, 3 units to an eight-fold dilution, etc. Different antigenic clusters are indicated with different colors as in **Figure** 1. Sera are shown with a grey outline, and serum names indicate the season of serum draw, e.g. S03 was drawn in 2002/2003. The shape of the symbol corresponds to the certainty in positioning of the virus or serum, and represents the coordination confidence area as locations on the map that the point could also occupy without increasing the stress of the map with more

than 0.5. The shape size typically increases as fewer HI titers are available. These maps were made without a minimum column basis.

Figure 3: Comparing antigenic maps based on ferret and human sera. A) Antigenic map based on 23 ferret sera, with the same virus set as **Figure 2** (made without minimum column basis), sera are shown in grey. B) Procrustes arrows from each virus point to its corresponding position in the human map in **Figure 2**.

Figure 4: Adding two additional sera to the human antigenic map. A) Antigenic map of the sera of the six high-responders plus two additional sera with titers of at least 240. B) Procrustes arrows displaying for each virus and serum in **Figure 4A** its corresponding position in **Figure 2**. C) Antigenic map of ferret data using the same virus set as in **Figure 4A**. D) Procrustes arrows showing the position of each virus in the ferret antigenic map of **Figure 4C** in the human antigenic map shown in **Figure 4A**.

Figure 5: Antibody landscapes [6] of the six high-responding human sera, displayed on the human antigenic map of **Figure 2**. Antibody titers of a serum (grey dots) are displayed along the z-axis, with higher titers, and higher regions of the antibody landscape, corresponding to high antibody levels in an individual.

FERRET SERA

BE/353/89
GU/54/89
NL/620/89
HK/34/90
VI/2/90
BE/32A/92
BE/32V/92
GD/25/93
NA/933/95
NL/47/95
NL/218/95
SP/1/96
SY/5A/97
NL/22/03
NL/88/03
WY/3/03
NY/55/04
WE/1/04
HI/52/05
BR/10/07
UR/716/07
NL/377/08
PE/16/09
VI/210/09

HUMAN SERA

S95-1
S95-2
S95-3
S95-4
S97-1
S98-1
S00-1
S00-2
S00-3
S00-4
S04-1
S04-2
S04-3
S05-1
S10-1
S10-2
S11-1

WE/5/89
VI/1/89
CA/1/91
BE/352/89
ST/7/92
FI/220/92
NL/938/92
SD/9/93
ST/20/93
JO/33/94
FI/381/95
WU/359/95
HK/280/97
SY/5/97
PM/2007/99
NL/1/02
FU/411/02
CF/7/04
WN/67/05
BR/10/07
PE/16/09
VI/361/11
NL/63/11

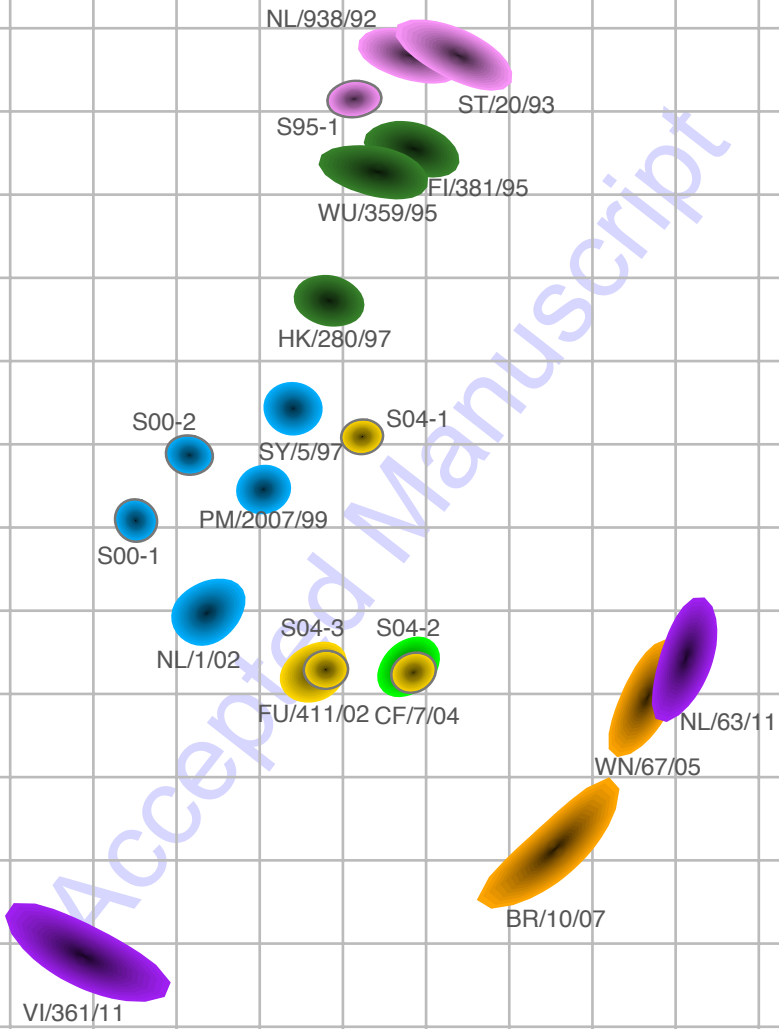

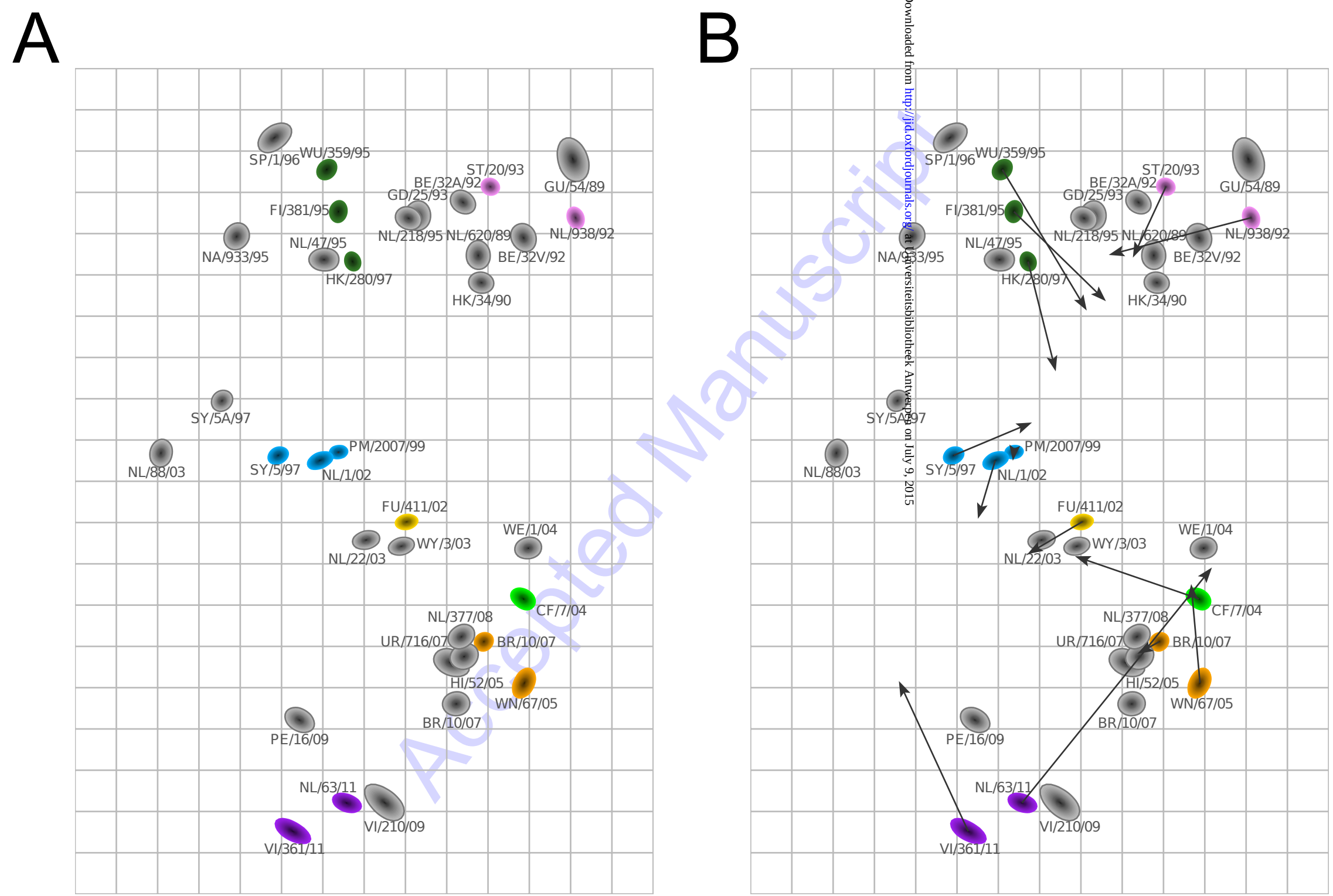

A

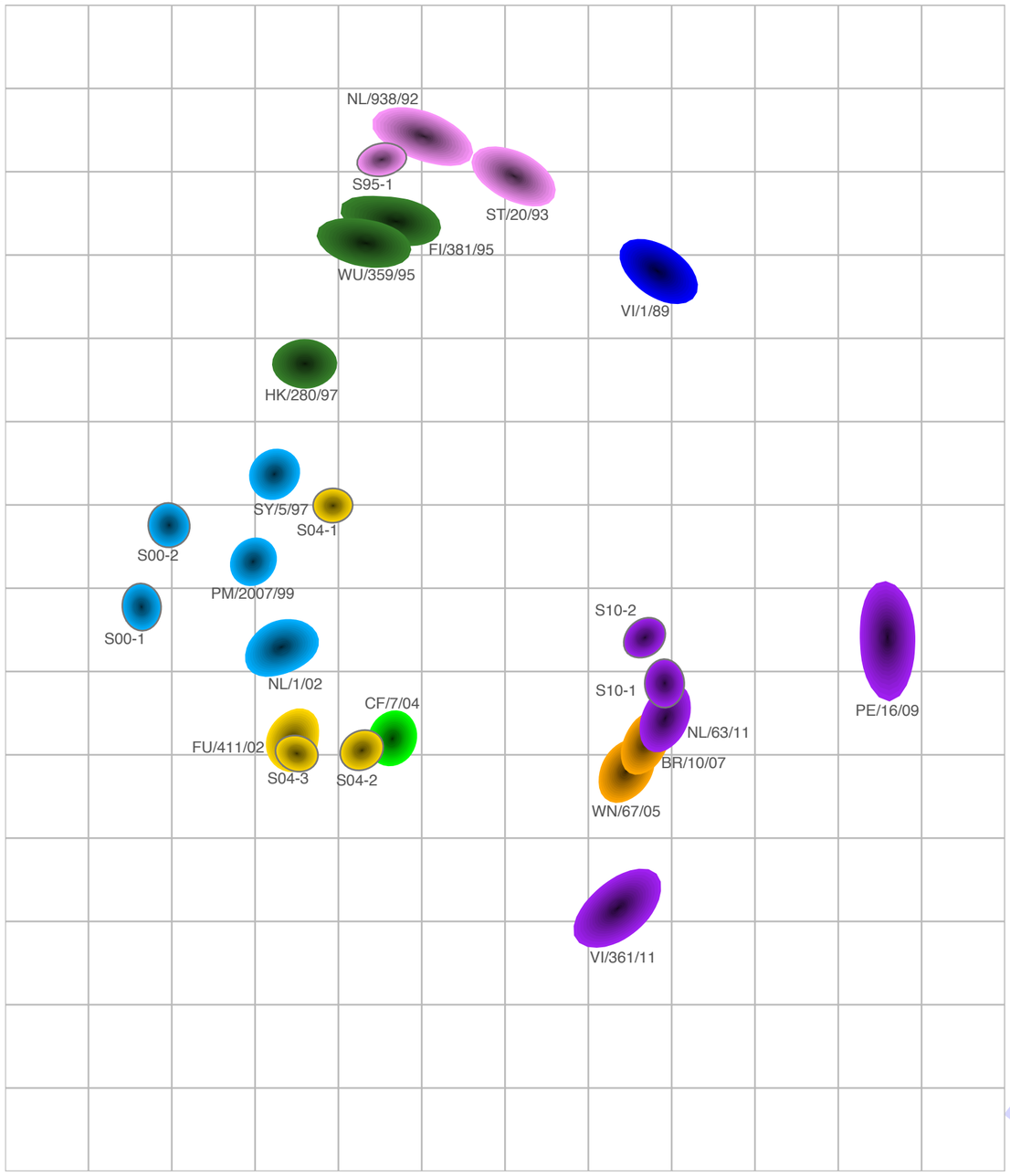

B

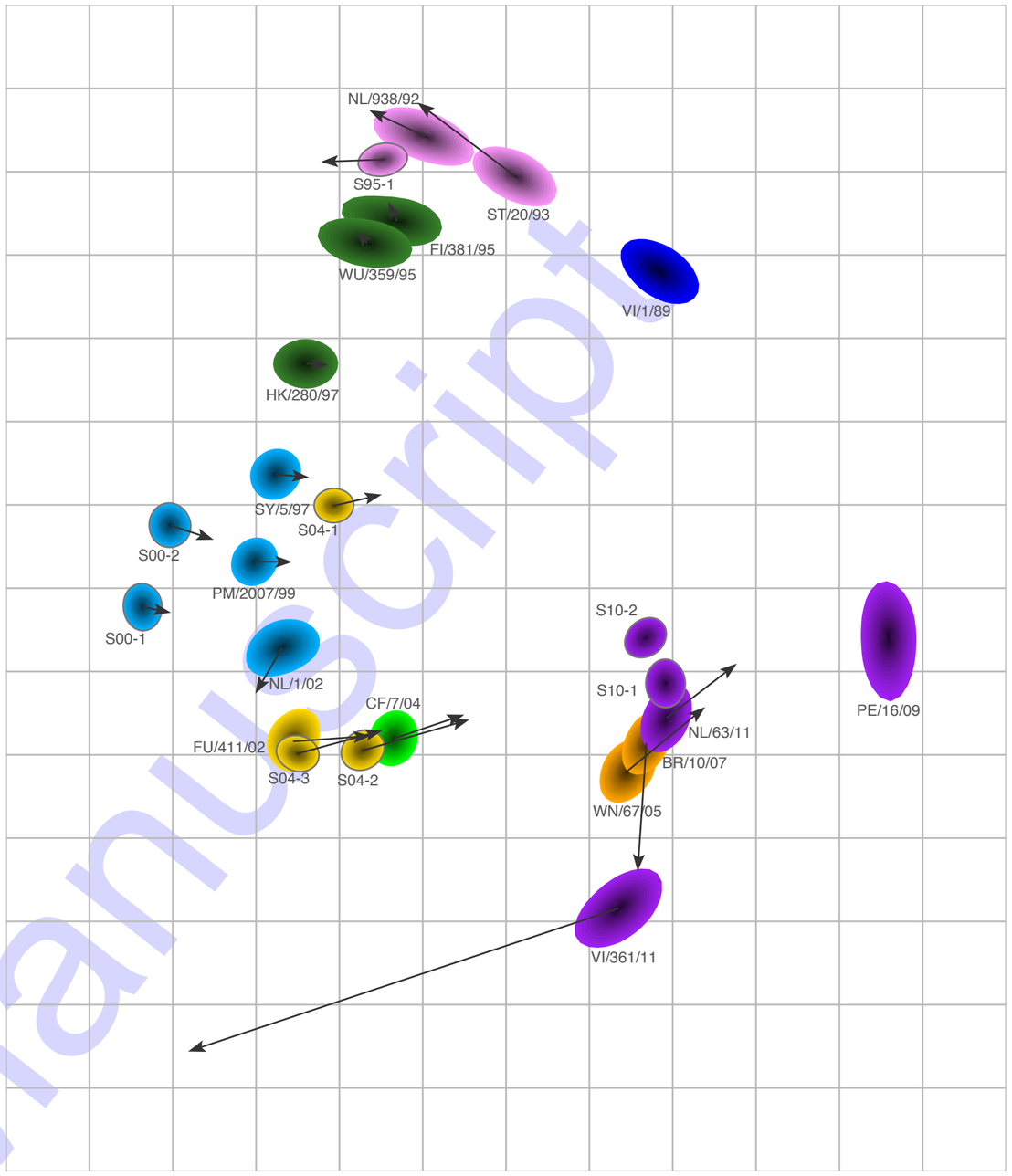

C

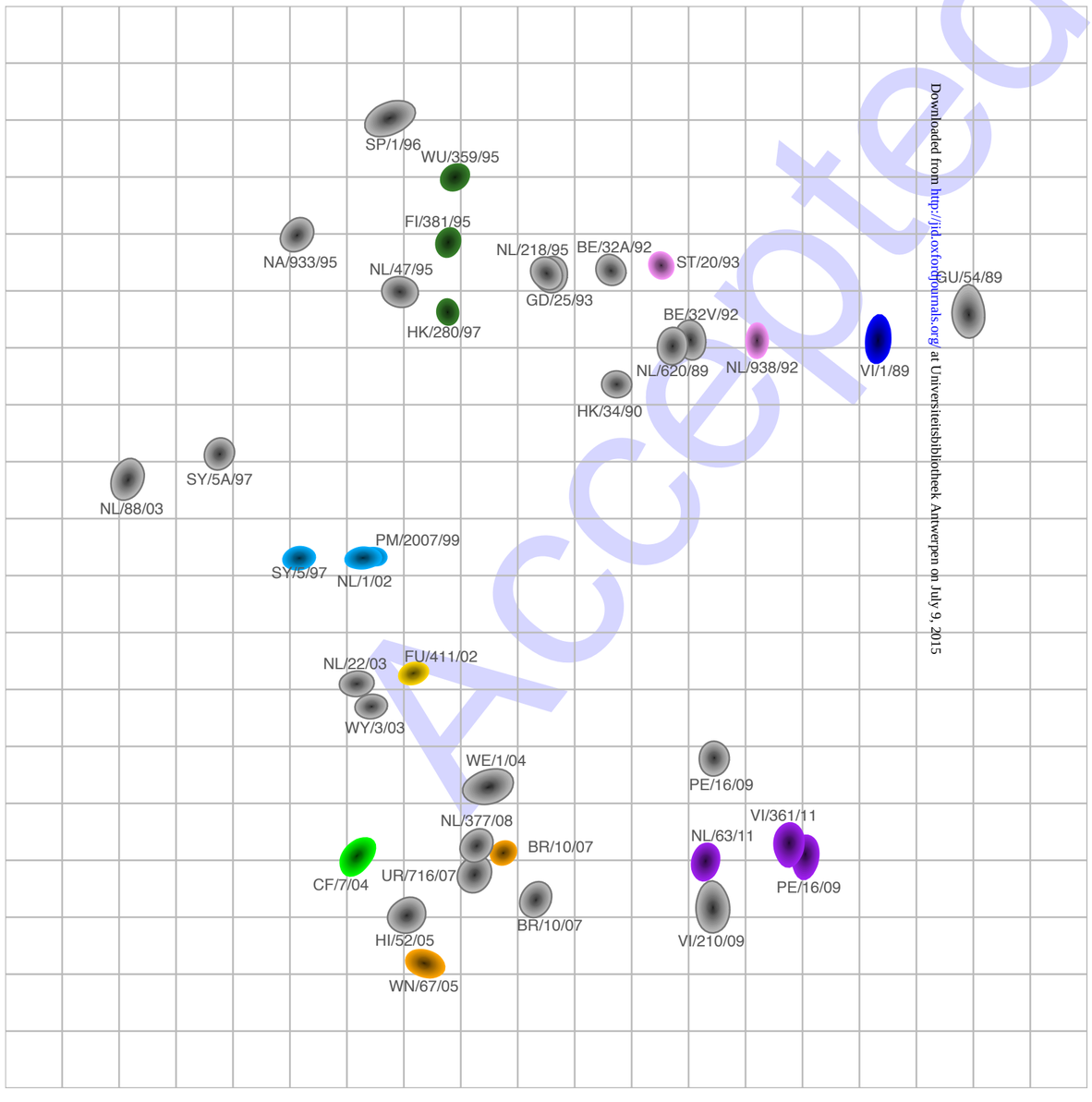

D

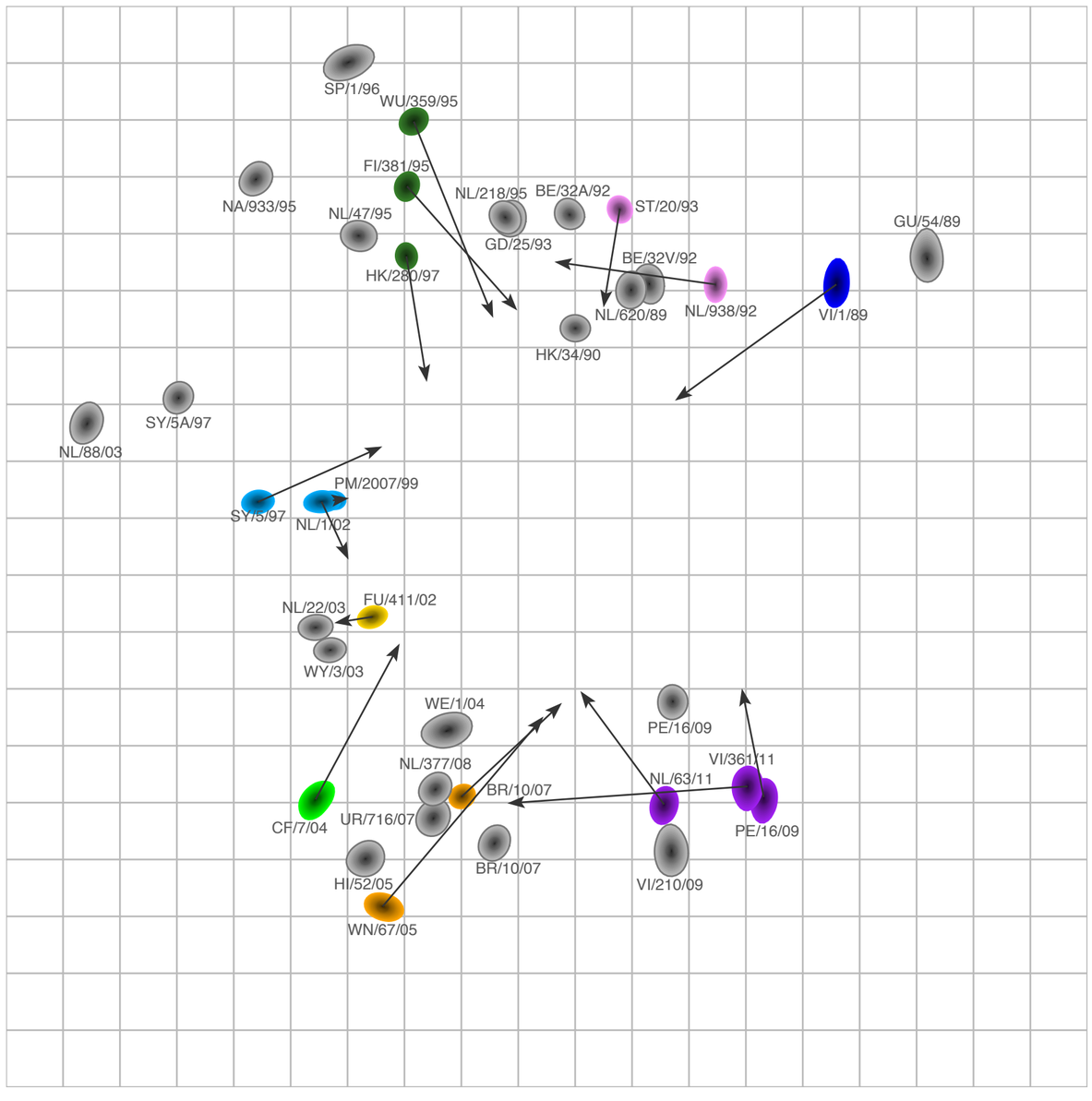

S95-1

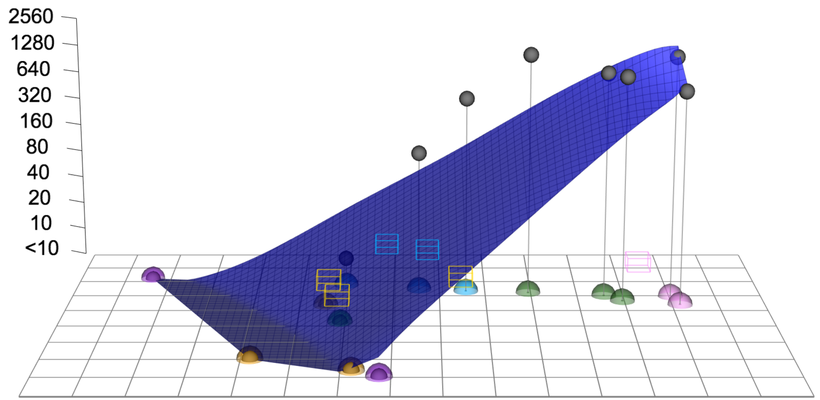

S00-1

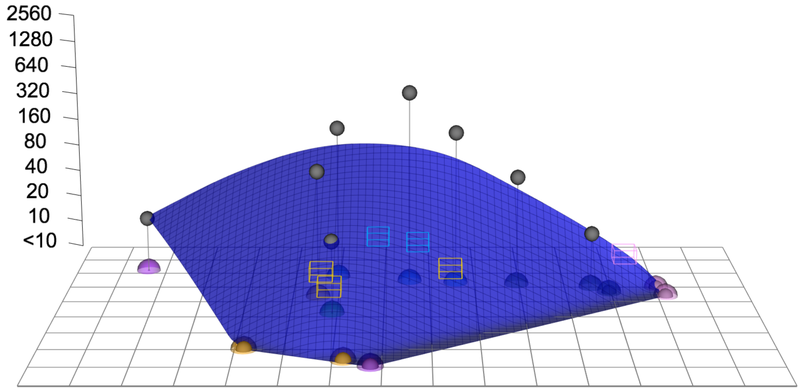

S00-2

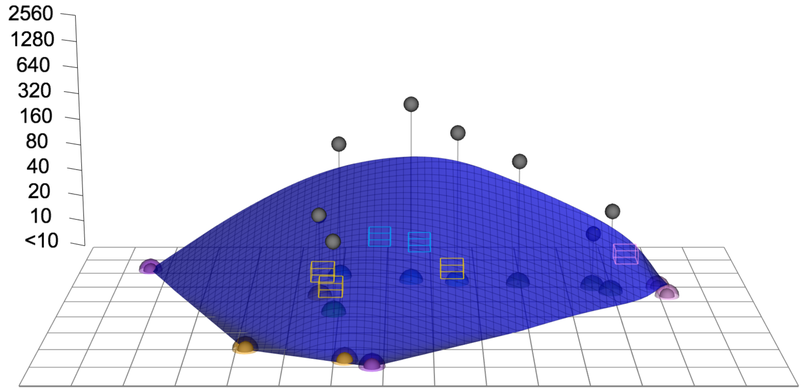

S04-1

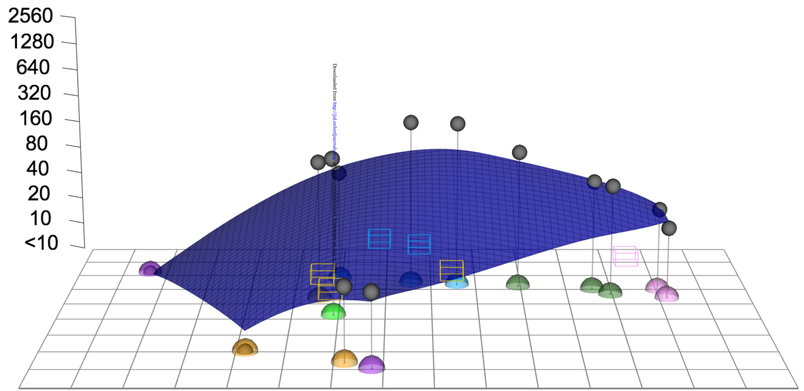

S04-2

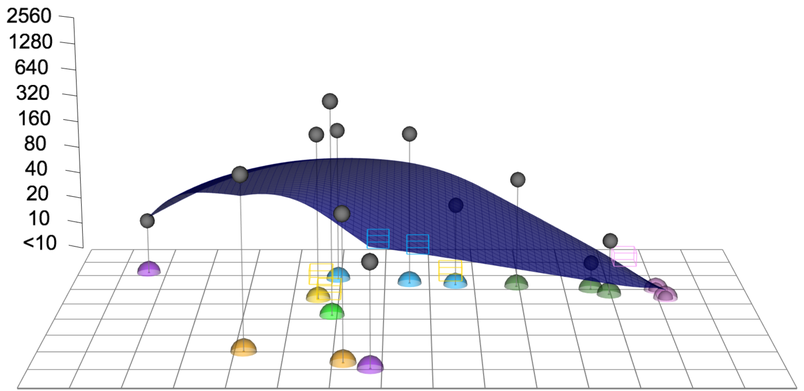

S04-3